

## Flat Far Field Lenses and Reflectors

Miguel Ruphuy, Zhao Ren, and Omar M. Ramahi\*

**Abstract**—We present a flat lens design that provides focusing with no aberration. By profiling the refractive index of the lens to generate a spherical wavefront at the exit side of the lens, the transmitted fields converge at a specified focal point. The focusing is achieved using primarily the dispersion phenomenon. We show through numerical examples that focusing without aberration can be achieved at a specific frequency and that focusing is possible over a narrow range of frequencies providing that the dispersion is minimal. Additionally, we show that the same principle used to design the lens can be used to design flat reflectors with a focal point focusing.

### 1. INTRODUCTION

The interest in constructing a perfect lens perhaps dates back centuries ago when lenses were first invented or even possibly when the laws of refraction were first conceived [1, 2]. The definition of a perfect lens, in fact, remain elusive. Here one has to make a distinction between near-field and far-field lenses. The seminal paper by Pendry [3] proposed a perfect lens in the sense that the complete propagating and evanescent spectra emanating from an object can be faithfully constructed at a distance from the object.

Whether the work of Pendry in [3] achieved a perfect lens or not continues to be debated [4–7]; however, the work ignited a remarkable enthusiasm in the quest for better optics and better focusing of electromagnetic waves in general. Due to fundamental material limitations such as dispersion and losses, the lens proposed by Pendry remains a theoretical construction at best. Nevertheless, even if the Pendry lens can be realized physically, it remains of limited utility since reconstructing the full spectrum can only be possible at a close distance (electrically) from the object.

More recently, a far-field lens, or a *superlens*, was proposed where the Pendry lens was used to enhance the evanescent spectrum coming out of the object and then a grating surface was used to convert the evanescent spectrum to a propagating one that can be detected in the far field [8, 9]. The far-field superlens introduced flexibility in near-field microscopy but remains limited as it would require a grating structure to be placed in the very close proximity of the object, which precludes full imaging (i.e., reconstitution of both propagation and evanescent spectra) of physically distant objects. Nevertheless, irrespective of whether one can convert the entire spectrum into traveling waves, reconstruction of the arriving propagating waves requires another lens (or a reflector) which has distinct challenges, most important of which is aberration [8, 9]. Aberration is a deformation in the image typically caused by the lens geometry in curved lenses. In the context of focusing of plane waves, aberration refers to the quality of convergence of a plane wave onto a single point. In most applications in the microwave frequency regime, minimizing aberration is not the highest concern, as high, but not perfect focusing is what is most desired. (High focusing is synonymous with high gain antennas such as arrays, apertures, reflectors, . . . , etc.). Additionally, in the microwave regime, the construction of a classical lens itself is a significant undertaking due to size and volume requirements.

---

Received 26 December 2013, Accepted 23 January 2014, Scheduled 30 January 2014

\* Corresponding author: Omar M. Ramahi (oramahi@uwaterloo.ca).

The authors are with the School of Electrical and Computer Engineering, University of Waterloo, Waterloo, Ontario N2L 3G1, Canada.

Therefore, one can infer that “perfection” in a lens is a rather relative term depending on whether one is transmitting or receiving. For instance, in the work of [8, 9], the detector has yet to construct the arriving spectrum faithfully in the sense that convergence of rays has to be “perfect”. If a classical convex lens is used for reception of the rays, then, even if dispersion is not of concern (since near-field microscopy is typically bandlimited), lens aberration remains a challenge.

Focusing can also be achieved using coordinates transformation by bending rays [10–12]. Wave bending is accomplished by a highly anisotropic medium where the medium material properties depend on its coordinate location. This discrete coordinate transformation technique [10] translates a 2D convex optical lens into a flat lens.

Another approach for designing flat lenses is the Fresnel zone plates. By proper design of the plates and using Huygens hypothesis, the secondary sources between the plates can be made to add up constructively at a far-field focal point (see [13]). Note that the primary mechanism behind the zone plates is diffraction; thus, the operation of the zone plate as a focusing lens can be predictable strictly in the far field zone. Yet another approach for designing flat lenses is the Gradient Index Lens (GRIN) technique [14–18]. In the GRIN lenses, the designs were based on ray bending and the assumption that the object produces rays that impinge on the lens at shallow angles and the focal point is distant from the lens (to warrant small angle approximation for the tangent function as in [14]). In GRIN techniques, the lens is sufficiently thick in terms of wavelengths to provide for ray bending within the lens medium.

Recently two different groups succeeded in creating a flat lens for focusing the far field [19–21]. Both groups used metallic inclusions, or very small antennas, to achieve a phase shift profile on the exit side of the lens such that the wavefront converges at a single focal point. These designs have losses and reflections, thus significantly reducing the focusing efficiency. Additionally, the focusing is limited to a very narrow band of frequencies which govern the design of the metallic inclusions responsible for the precise phase shift profile throughout the lens. In essence, the focusing is achieved by exploiting and carefully tailoring the resonance of the metallic inclusions.

Clearly, refraction, diffraction, coordinates transformation and resonance were all exploited in the quest for the ultimate focusing. In this work, we present theoretical findings behind a focusing technique that is based on dispersion [29]. We limit our work to far-field focusing (i.e., focusing of an incident plane wave arriving from infinity onto a specific focal point in the proximity of the lens).

## 2. DESIGN METHODOLOGY

The flat lens proposed here consists of multiple concentric annular rings with a radial refractive index profile as shown in Figure 1. The refractive index is realized using a dielectric material. Consider Figure 1 where the lens is positioned in the  $x$ - $y$  plane. A plane wave is assumed incident on the lens from the left hand side with a propagation vector in the  $+z$  direction. The incident plane wave propagates parallel to the normal of the lens with a uniform phase front at  $z = 0$ . To achieve focusing, i.e., ray convergence at a specified focal point, labeled as  $F$  in Figure 1, we require that the two ray trajectories ABE and CDE have equivalent optical paths, or, equivalently, that the two rays impinging on A and C experience identical phase shift from the instant they enter the plate ( $z = 0$ ) to the instant they arrive at  $F$  (see Figure 2). Notice that the propagation vector of the incident wave is in the  $+z$  direction which is parallel to the boundaries of the dielectric rings. Therefore, by modeling the incident field as a composition of rays, no diffraction takes place as the rays impinge upon the rings, of course, aside from the interaction of the incident rays with the outer boundary of the outermost ring.

Continuing on with the ray model for the incident plane wave, each ray traveling through each ring experiences a phase shift of  $n_m k_o d$ , where  $n_m$  is the refractive index of the  $m$ th ring given by  $\sqrt{\epsilon_m \mu_m}$  and  $k_o$  is the free space wave number.  $m$  designates the ring number starting with  $m = 1$  corresponding to the center disk at  $x = y = z = 0$  and  $m = M$  corresponding to the outermost ring. Setting the phase shift of the two paths ABE and CDE to be identical gives:

$$n_1 k_o d + k_o F = n_m k_o d + k_o h_m \quad (1)$$

where  $h_m$  is the distance from the focal point to the middle of the  $m$ th ring.

The first term in Eq. (1) is the phase shift the incident wave experiences as it travels across the center ring and through free space to the focal point  $F$ . The second term corresponds to the phase shift

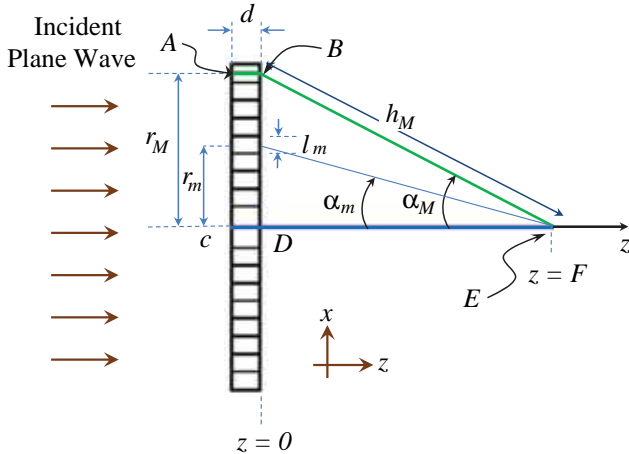


**Figure 1.** Cross-section view of the lens schematic in  $y = 0$  plane.

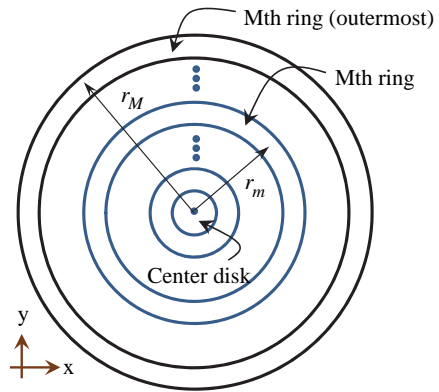


**Figure 2.** Cross-section view of the lens schematic in the  $z = 0$  plane.

across the  $m$ th ring and to the focal point.

Eliminating  $k_0$  from both sides of Eq. (1), we have

$$n_1 d + F = n_m d + h_m \tag{2}$$

which gives the design equation for  $n_m$  in terms of  $n_1$  or vice versa.

By selecting the refractive index of any of the  $M$  rings, the refractive index of all other rings is fixed via Eq. (2). Expressed in terms of the angle  $\alpha_m$ , we have

$$n_1 = n_m + \frac{F}{d} \left( \frac{1}{\cos(\alpha_m)} - 1 \right) \tag{3}$$

Once  $n_M$  and  $n_1$  are fixed, the refractive indexes of the remaining ring will be selected according to Eq. (3). The number of rings  $M$  will only dictate the resolution of the lens.

If the dielectric material used has low dependence on frequency, at least over a specific frequency range, Eq. (3), similarly, will have low dependence on the frequency over the same frequency range.

In earlier works [23–25], it was demonstrated that a gradient index microwave lens can increase the gain of horn antennas by focusing the beam. In fact, Eq. (9) of [25] reduces to Eq. (3) above. It is interesting that reference [25] arrived at an equation identical to (3) using a different approach involving differential calculus, whereas our derivation was based on convergence of rays and equivalence of optical paths. What is important to notice, however, is that in Eq. (3) of [25], the authors do not consider multiple reflections inside the lens. Their thick lens creates actual cavities which generates modes and unpredicted behaviors. Additionally, there is a coupling effect (addressed later on) between adjacent layers which is not negligible for lenses comparable or thicker than a wavelength as the case presented in [25]. In our work, however, the derivation was based on building an electrically thin lens. This design criteria allows to assume reasonably that the waves at each layer are confined and will not reflect on the interface between layers, thus achieving zero monochromatic aberration, characteristic that could not be achieved with [25] methodology. Furthermore, to account for the diffraction given by the lens edges, the refractive index of the  $M$ th is chosen equal to 1. This means that vacuum is actually accounted as an additional layer.

To test the validity of Eq. (2), we consider, as an example, a lens with a radius and focal length of  $4\lambda_0$ . We consider these two parameters as the primary design parameters. The remaining lens parameters such as the thickness of the lens,  $d$ , the width of the dielectric rings,  $l_m$  and the lens dielectric medium parameters, can all be chosen with some flexibility. To start, we fix the refractive index of the outermost ring at  $n_M = 1$ . The lens depth  $d$  needs to be electrically small in order to preserve the ray-like behavior of the incident field as it penetrates the lens. For the example chosen

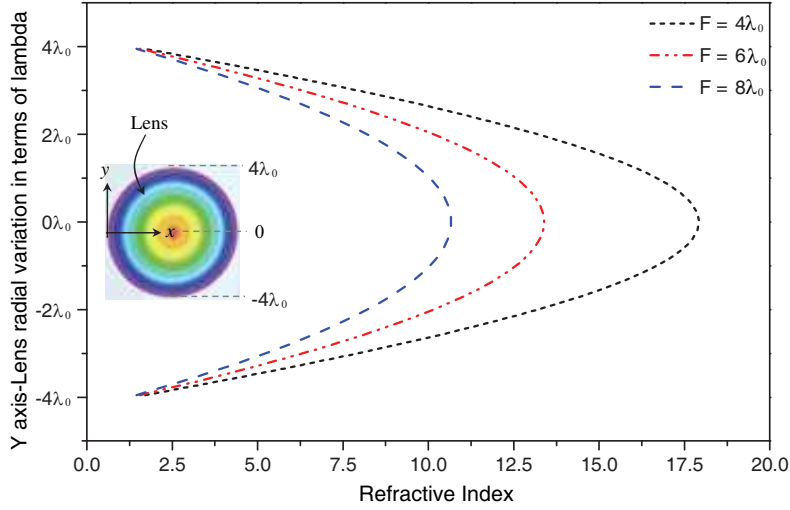


**Figure 3.** The refractive index profile along the radial direction for a lens with  $d = \lambda_o/10$  and  $4\lambda_o$  radius.

here, we set  $d = \lambda_o/10$ , where  $\lambda_o$  is the free-space wavelength. We show in Figure 3 the calculated refractive index profile along the  $y$  axis (or the radial) of the  $\lambda_o/10$  thick lens for three different focal lengths.

Notice that the design equation provide a degree of flexibility in terms of the profile of the refractive index and also the selection for the relative permittivity and permeability for each annular ring. In fact, such flexibility allow for choosing the permeability and permittivity equal to achieve impedance matching for the incident wave and eliminate reflections which in turn helps increase the focusing efficiency considerably. This design flexibility that allows for the possibility of impedance matching can be viewed as a contrast to previous flat lens designs that necessitated the use of thin film to minimize reflections which in turn confine the lens operation to a narrow frequency band.

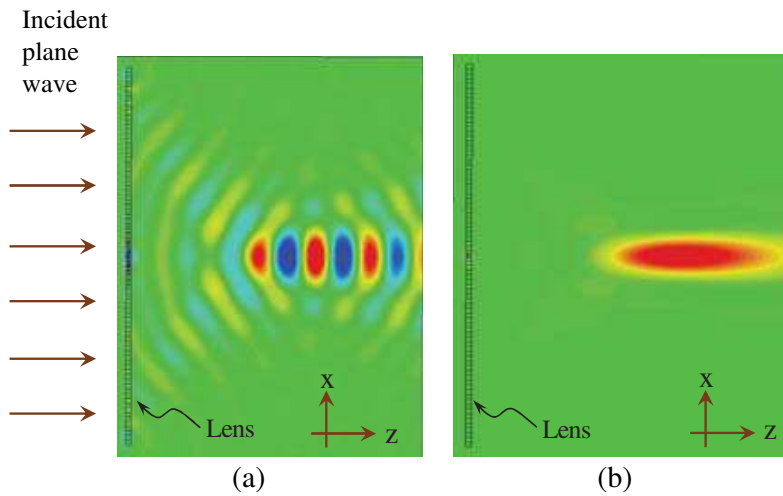


**Figure 4.** (a) Magnitude of the Total Electric Field over the  $y = 0$  plane. Color scale extends from  $-6.85$  V/m (deep blue) to  $6.85$  V/m (deep red). (b) Magnitude of the  $z$ -directed Poynting vector over the  $y = 0$  plane. Color scale extends from  $0$  VA/m<sup>2</sup> (green) to  $0.202$  VA/m<sup>2</sup> (deep red).

We used the full-wave electromagnetic simulation tool CST to simulate the performance of the lens. Figure 4 shows the total electric field magnitude distribution over the  $y = 0$  plane for a plane wave incident from  $z = -\infty$  and for a fixed instant in time. Clearly visible in the figure the spherical

wavefronts generated on the right-hand side of the lens on both sides of the focal point as the waves converge and then start diverging as they leave the focal point. Figure 4(b), shows the magnitude of the  $z$ -directed Poynting vector, demonstrating high power concentration within close proximity of the focal point. Figure 5 shows the power distribution along the  $z = 4\lambda_o$  plane where the design's focal point is located. Figure 5 shows a normalized contour plot of the Poynting vector at the  $z = 4\lambda_o$  plane.

Note that Eq. (2) indicates that the rings' design, and consequently the focusing depended slightly on the frequency as long as the refractive indexes of the rings used to construct the lens varied slightly with frequency. We emphasize, however, that our design, namely Eq. (2), was based on the assumption that a ray enters each of the annular rings and experiences a phase shift as it propagates through the lens along the  $+z$  direction. If the thickness of the lens is increased, or alternately, is no longer electrically small, we expect coupling to take place between adjacent rings in a manner highly similar to coupling between closely spaced transmission lines [26,27]. If the lens width increases, then the coupling can increase to sufficiently disturb the phase profile that was designed for at the exit side of the lens at  $z = d$ . From an optical point of view, the longer the path  $d$ , the larger the spreading of the wave, and hence the higher coupling between adjacent rings. If the coupling between adjacent layers increases, which would be the case when the thickness of the lens increases, the phase profile on the right-hand-side ( $z = 0$  in Figure 1) would be different from what we designed for, thus leading to a type of aberration or de-focusing. Therefore, even under the assumption that *each* ring has minimal or even zero dispersion, it should be kept in mind that the design equation was based on the assumption that each ray entering a ring is confined to that ring until its exit. While a theoretical analysis to gauge the effect of the coupling cannot be foreseen at this time, the effect of such coupling, if needed, can be gauged numerically.

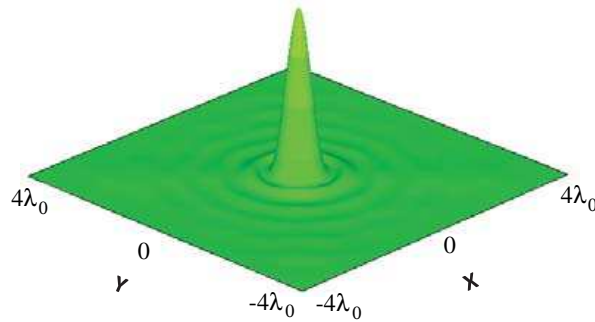


**Figure 5.** Magnitude of the normalized  $z$ -directed Poynting vector over the  $z = 4\lambda_o$  plane.

### 3. FLAT REFLECTORS

The same strategy for inducing a scattered field that focuses at a specific point can be used to design a reflector that would focus the field at a specific focal point. Such reflector would perform the function of a paraboloid (dish reflector) as shown in Figure 6. The reflector can be designed using the same principle of requiring the rays of an incident field that arrive normal to the reflector to scatter at different angles and converge at a focal point. The primary difference from the lens, however, is that the dielectric rings are now backed by a perfectly conducting sheet (at  $z = -d$ ) as shown in Figure 7, thus forcing the incident ray to traverse the lens twice. Referring to Figure 7, the design equation for the reflector is given by

$$n_1 = n_m + \frac{F}{2d} \left( \frac{1}{\cos(\alpha_m)} - 1 \right) \tag{4}$$

To validate the reflector design, we consider a reflector disk with a radius and focal length of  $4\lambda_o$ . The thickness of the reflector would be half that of the lens designed earlier. A perfectly conducting plate is positioned behind the dielectric multi-ring disk. Similar to the lens case, the incident plane wave arrives at the surface of the lens with uniform phase, it then propagate through the lens a round trip exiting with a phase profile designed to achieve convergence at the focal length. Figure 8(a) shows the

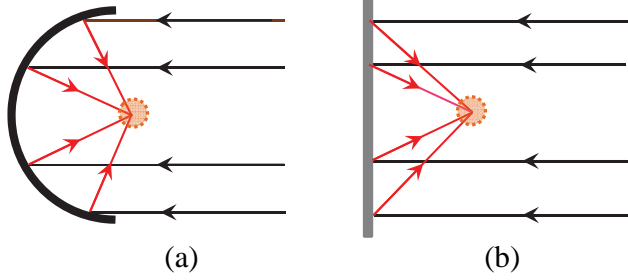


**Figure 6.** (a) Cross-section at the center of a classical paraboloid reflector. (b) Cross-section of a flat focusing reflector proposed in this paper.

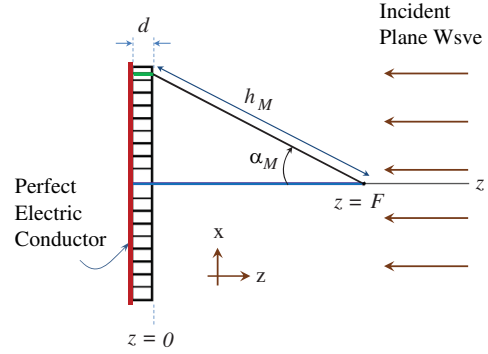


**Figure 7.** Schematic showing the cross-section of the reflector in the  $y = 0$  plane.

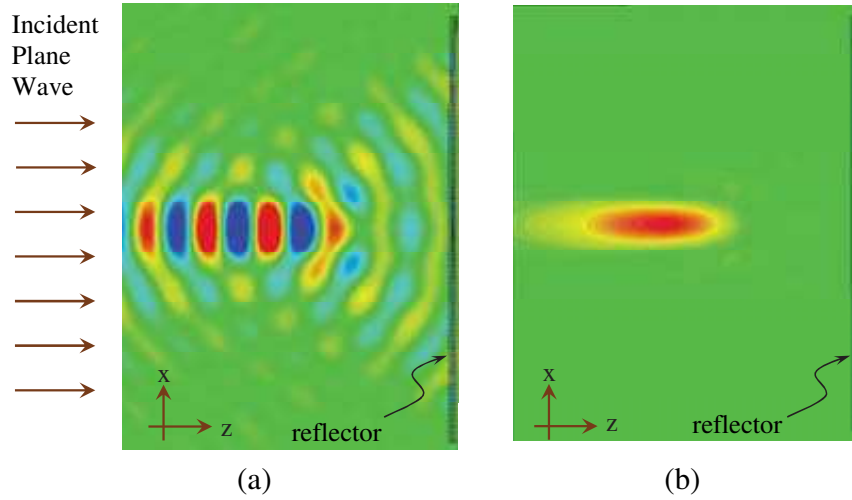


**Figure 8.** (a) Magnitude of the scattered electric field over the  $y = 0$  plane. Color scale extends from  $-5.11$  V/m (deep blue) to  $5.11$  V/m (deep red). (b) Magnitude of the  $z$ -directed Poynting vector over the  $y = 0$  plane. Color scale extends from  $0$  VA/m<sup>2</sup> (green) to  $0.239$  VA/m<sup>2</sup> (deep red).

scattered electric field distribution on the  $y = 0$  plane. The profile of a spherical wavefront imploding at the focal point is visible. Figure 8(b) shows the  $z$ -directed Poynting vector on the same plane of  $y = 0$ ; again showing strong concentration of the scattered field.

#### 4. CONCLUSION

In conclusion, we presented a thin flat lens based on designing the refractive index to achieve a phase profile sufficient for ray convergence at a specified focal point. The design is based on the assumption that the lens is electrically thin, thus being fundamentally different from gradient-index techniques which bend the rays *within* an electrically-thick lens [22]. A numerical example was presented where aberration-free focusing was achieved at a specific focal point. The design provides the flexibility of not requiring the focal point to be in the far field.

Because of the ray behavior assumption of the field interaction with the dielectric layers of the lens, the design is most suitable for large aperture lenses. Furthermore, using the same methodology presented here for lens design, a flat reflector can be designed with a focal point. The results presented in this paper were purely based on full-wave electromagnetic simulation. For the examples presented,

the dielectric material needed for building the lens and reflector requires the availability of a material with refractive index ranging from 1 to 18. To minimize reflection, the permeability and permittivity can be chosen to be equal to the refractive index.

The practical realization of the flat lens and reflector proposed here will largely depend on the promise of metamaterials to realize refractive indices as high as 20. In a very recent article, metamaterial with very high index of refraction (exceeding 20) was developed and tested experimentally in the THz regime and even microwave frequencies [28]. Alternatively, high dielectric constant materials can be used in microwave regime. Custom made dielectrics with permittivities as high as 30 are under development. Indeed the development of such material holds the key to a practical realization of the flat lens proposed here which can have significant impact on lens design in general and dish antennas used for space applications.

## ACKNOWLEDGMENT

The authors acknowledge with deep gratitude the financial support of MICIT/CONICIT, UCR and the Natural Sciences and Engineering Research Council (NSERC) of Canada.

## REFERENCES

1. Zghal, M., H.-E. Bouali, Z. B. Lakhdar, and H. Hamam, "The first steps for learning optics: Ibn Sahl, Al-Haythams and Youngs works on refraction as typical examples," *The Education and Training in Optics and Photonics Conference (ETOP) 2007*, Ottawa, Ontario, Canada, 2007.
2. King, H. C., *The History of the Telescope*, Courier Dover Publications, 2003.
3. Pendry, J. B., "Negative refraction makes a perfect lens," *Phys. Rev. Lett.*, Vol. 85, 3966–3969, 2000.
4. Williams, J. M., "Some problems with negative refraction," *Phys. Rev. Lett.*, Vol. 87, 249703-1, 2001.
5. Pendry, J., "Pendry replies to Williams," *Phys. Rev. Lett.*, Vol. 87, 249704-1, 2001.
6. Pendry, J., "Pendry's reply to Hooft," *Phys. Rev. Lett.*, Vol. 87, 249702-1, 2001.
7. Walser, R. M., A. P. Valanju, and P. M. Valanju, "Comment on extremely low frequency plasmons in metallic mesostructures," *Phys. Rev. Lett.*, Vol. 87, 119701-1, 2001.
8. Jacob, Z., L. V. Alekseyev, and E. Narimanov, "Optical Hyperlens: Far-field imaging beyond the diffraction limit," *Opt. Express*, Vol. 14, 18, 2006.
9. Liu, Z., S. Durant, H. Lee, Y. Pikus, Y. Xiong, C. Sun, and X. Zhang, "Development of optical hyperlens for imaging below the diffraction limit," *Nano. Lett.*, Vol. 7, 403–408, 2007.
10. Yang, R., W. Tang, Y. Hao, and I. Youngs, "A coordinate transformation-based broadband flat lens via microstrip array," *IEEE Antennas Wireless Propagat. Lett.*, Vol. 10, 99–102, 2011.
11. Pendry, J. B., D. Schurig, and D. R. Smith, "Controlling electromagnetic fields" *Science*, Vol. 312, 1780–1782, 2006.
12. Kwon, D. H. and D. H. Werner, "Transformation optical designs for wave collimators, flat lenses and right-angle bends," *New J. Phys.*, Vol. 10, 115023, 2008.
13. Sussman, M., "Elementary diffraction theory of zone plates," *Am. J. Phys.*, Vol. 28, 394–398, 1960.
14. Wood, R. W., *Physical Optics*, The Macmillan Company, 1905.
15. Sands, P. J., "Third-order aberrations of inhomogeneous lenses," *J. Opt. Soc. Am.*, Vol. 60, 1436–1443, 1970.
16. Sands, P. J., "Inhomogeneous lenses, III. Paraxial optics," *J. Opt. Soc. Am.*, Vol. 61, 879–885, 1971.
17. Bass, M., Ed., *Handbook of Optics*, 3rd Edition, The McGraw-Hill Companies, 2010.
18. Ilyas, S. and M. Gal, "Gradient refractive index planar microlens in Si using porous silicon," *Appl. Phys. Lett.*, Vol. 89, 211123-3, 2006.

19. Aieta, F., P. Genevet, M. A. Kats, N. Yu, R. Blanchard, Z. Gaburro, and F. Capasso, "Aberration-free ultrathin flat lenses and axicons at telecom wavelengths based on plasmonic metasurfaces," *Nano Letters*, Vol. 12, 4932–4936, 2012.
20. Yu, N., P. Genevet, M. A. Kats, F. Aieta, J. P. Tetienne, F. Capasso, and Z. Gaburro, "Light propagation with phase discontinuities: Generalized laws of reflection and refraction," *Science*, Vol. 334, 333–337, 2011.
21. Chen, X., L. Huang, H. Muhlenbernd, G. Li, B. Bai, Q. Tan, G. Jin, C. W. Qiu, S. Zhang, and T. Zentgraf, "Dual-polarity plasmonic metalens for visible light," *Nature Communications*, Vol. 3, Article No. 1198, 2012, doi:10.1038/ncomms2207.
22. Liu, R., Q. Cheng, J. Y. Chin, J. J. Mock, T. J. Cui, and D. R. Smith, "Broadband gradient index microwave quasi-optical elements based on non-resonant metamaterials," *Opt. Express*, Vol. 17, 21030–21041, 2009.
23. Ma, H. F., X. Chen, H. S. Xu, X. M. Yan, W. X. Jiang, and T. J. Cui, "Experiments on high-performance beam-scanning antennas made of gradient-index metamaterials," *Appl. Phys. Lett.*, Vol. 95, 094107, 2009.
24. Chen, X., H. F. Ma, X. Y. Zou, W. X. Jiang, and T. J. Cui, "Three-dimensional broadband and high-directivity lens antenna made of metamaterials," *J. Appl. Phys.*, Vol. 110, 044904-8, 2011.
25. Ma, H. F., X. Chen, X. M. Yang, W. X. Jiang, and T. J. Cui, "Design of multibeam scanning antennas with high gains and low sidelobes using gradient-index metamaterials," *J. Appl. Phys.*, Vol. 107, 014902-9, 2010.
26. Bakoglu, H., *Circuits, Interconnections, and Packaging for VLSI*, Addison-Wesley, 1990.
27. Kabiri, A., Q. He, M. Kermani, and O. M. Ramahi, "Design of a controllable delay line," *IEEE Trans. Advanced Packaging*, Vol. 33, 1080–1087, 2010.
28. Choi, M., S. H. Lee, Y. Kim, S. B. Kang, J. Shin, M. H. Kwak, K-Y. Kang, Y-H. Lee, N. Park, and B. Min, "A terahertz metamaterial with unnaturally high refractive index," *Nature*, Vol. 470, 369–373, 2011.
29. Ramahi, O. M. and M. Ruphuy, "Flat lenses and reflectors and method for construction," Patent Application No. US61912634, 2010.